Testing the effects of TDP-43 on NPTX2 levels during neuronal differentiation

Report of the 1st rotation project No. 6 of BIO328 Neurobiology

Place:
Laboratory of Prof. Dr. Magdalini Polymenidou

Date of submission:
22.03.2023

Submitted by:

David E. Hogg

Veronika Voskresenska

Supervisor:
Beatrice Gatta (PhD student)

Department of Quantitative Biomedicine University of Zurich

Abstract

The abnormal aggregation of proteins is a key feature in most neurodegenerative diseases, including amyotrophic lateral sclerosis (ALS) and frontotemporal dementia (FTD). Specific subgroups of these two fatal disorders share some clinical features with each other, pointing to their undeniable relation. There is a growing amount of scientific and clinical evidence showing the significance of mutations in RNA binding proteins (RBPs) leading to an increased risk of developing neurological diseases such as ALS and FTD. These diseases are characterized by alterations in RNA metabolism due to loss of function caused by protein mislocalization and gain of neurotoxicity from accumulated pathological protein aggregates. The TAR DNA binding protein of 43 kDa (TDP-43) is the main aggregating protein involved in known clinical cases of ALS and various forms of FTD. The study of TDP-43 proteinopathies demands human cellular models, as it involves human-specific mechanisms in which neurons are the cell-type affected in pathology. Previous results in self-organized multicellular neural cultures overexpressing TDP-43, showed that as a consequence of TDP-43 alteration, the synaptic protein NPTX2 also start to misaccumulates into the cytoplasm; notably this event is also observed in ALS and FTD patient neurons. Therefore, a new pathway of toxicity has been identified in which TDP-43 pathology is linked to NPTX2 misaccumulation in mature neurons overexpressing TDP-43 and neurons of ALS/FTD patients. However, the link between TDP-43 and NPTX2 as well as the mechanisms underlying neurotoxicity in ALS/FTD pathology are yet to be well-defined. One interesting question that still needs to be addressed is what the impact of TDP-43 on NPTX2 levels also during neuronal differentiation. Therefore, in this project we aim at investigating how TDP-43 can regulate NPTX2 levels in differentiating neurons.

Introduction

Pathogenic deposits containing TAR DNA-binding protein 43 (TDP-43) are present in the brain and spinal cord of patients across a spectrum of neurodegenerative diseases. For example, up to 97% of patients with sporadic amyotrophic lateral sclerosis and roughly 45% of patients with frontotemporal lobar degeneration exhibit TDP-43 positive neuronal inclusions, indicating a potential role for this protein in disease pathogenesis. Although TDP-43 is an essential RNA/DNA binding protein critical for RNA-related metabolism, uncovering the pathophysiological mechanisms through which TDP-43 mediates neurodegeneration appears complex, and understanding these molecular processes is crucial for the development of effective therapies (De Boer et al., 2021).

Amyotrophic lateral sclerosis (ALS)

Amyothropic lateral sclerosis (ALS) is a motor system neurodegenerative disease in which upper as well as lower motor neurons are progressively lost (Geser et al., 2010). Due to this progressing loss of motor neurons, the muscles are being degraded which causes muscle

atrophy and weakness and ultimately leads to the paralysis of muscles and lungs, resulting in death by suffocation (Mitchell & Borasio, 2007). This degeneration process is not only very aggressive, but ALS is also the most common adult motor system degenerative disease with a prevalence of 5.4 per 100'000 and incidence of 2 per 100'000 persons (Van Damme & Robberecht, 2009; Mejzini et al., 2019). Despite these metrics, it is yet unknown what the driving mechanism of action of the disease is and multiple hypotheses about the cause of ALS remain under investigation. Currently, the only treatment possible is symptom management and respiratory support via the drugs Riluzole and Edaravone, but the beneficial effects are within limits and scarce (Mejzini et al., 2019). Due to this gap in our knowledge, an effective treatment against ALS is lacking and we cannot treat the progressing loss of motor neurons and muscles. Apart from the degeneration of upper and lower motor neurons, a heterogenous spectrum of cytoplasmic inclusions have been observed and are now diagnostic for ALS, such as filamentous aggregations and small granules (Geser et al., 2010). In line with the observation of such inclusions, it is now suggested that ALS, among other neurodegenerative diseases such as Alzheimer's disease and Parkinson's disease, is a manifestation of a TDP-43 proteinopathy.
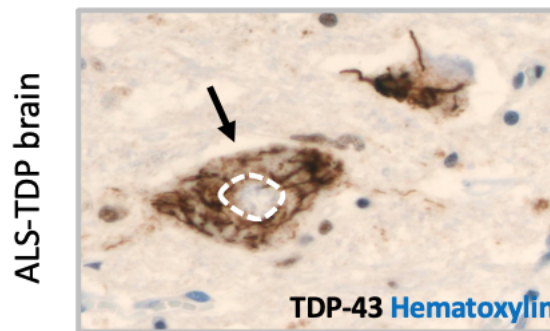

Fig 1: ALS TDP-43 patient brain section: dotted line shows the nuclear clearance, and the arrow shows toxic cytoplasmic aggregation of TDP-43 (Ling et al., 2013).

Frontotemporal dementia (FTD)

Frontotemporal dementia (FTD) is a very heterogenous disorder in which synapses and neurons in the frontal and temporal lobe of the brain are being degraded, resulting in cognitive and behavioral symptoms (Ling et al., 2013). FTD, like ALS, is also characterized by distinct protein aggregations with a preferred location in the brain's anatomy, like cortical cell layer and cell type (Younes and Miller, 2020). Clinical syndromes are associated with structural changes in the brain on a micro- and macroscopic level, such as the aforementioned loss of neurons. This progressive atrophy is described in four stages correlated with disease duration and dementia severity (Younes and Miller, 2020): Stage 1 initially involves atrophy in the anterior frontal cortex and the hippocampus, which then expands to the orbitofrontal gyrus, the basal ganglia and the posterior temporal lobe in stage 2. Stage 3 further worsens the frontal and temporal atrophy and leads to white matter involvement and the subsequent stage 4 encompasses severe atrophy in thalamic and all aforementioned regions. The term

itself stands for multiple neurological disorders in which one can observe behavioral changes, changes in language, changes in executive control and often also motor symptoms (Olney et al., 2018). Indeed, about 15% of FTP patients develop clinical symptoms such as motor system degeneration which are in line with ALS and about 15% of ALS patients have accompanying symptoms of behavioral or cognitive impairment (Ling et al., 2013). But contrary to ALS, the percentage of patients with a familial history of FTD (up to 50%) suggests a stronger genetic contribution. However, this suggests that the two diseases are linked not only clinically, but also pathologically and mechanically. And indeed, much like ALS, FTD is now also suggested to be a TDP-43 proteinopathy (Geser et al., 2010).
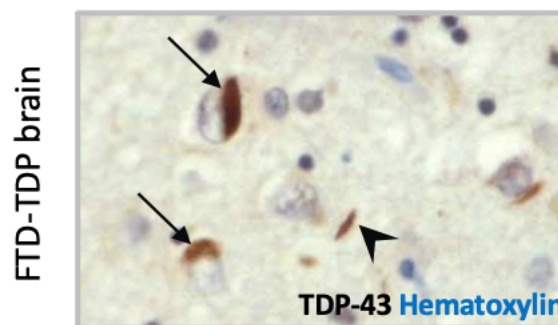

Fig 2: FTD patient brain section: arrows and arrows' head show nuclear clearance and toxic cytoplasmic aggregation of TDP-43 (Laferrière et al., 2019).

TDP-43 proteinopathies

TAR DNA-binding protein 43 (TDP-43, transactive response DNA binding protein 43 kDa) was primarily described as a suppressor of HIV-1 (HIV-1) gene expression. TDP-43 is responsible for numerous critical functions including regulation of RNA metabolism, mRNA transport, microRNA maturation and stress granule formation (Prasad et al., 2019). TDP-43 is mainly localized in the nucleus, however, it is involved in both nuclear and cytoplasmic processes and can translocate between these two compartments. TDP-43 plays a crucial role in the normal development of central neuronal cells during the early stages of embryogenesis, which is relevant to brain function (Wu et al., 2010). Given TDP-43's significant involvement in cellular processes, particularly in the development of the central nervous system, it is not surprising that the malfunction of TDP-43-related pathways has increasingly been acknowledged as a critical pathogenic mechanism in neurodegenerative disease (Sephton et al., 2010). The presence of hyperphosphorylated and ubiquitinated TDP-43 cytoplasmic inclusions has been identified as a pathological feature in both amyotrophic lateral sclerosis (ALS) and frontotemporal lobar disease (FTD). Pathogenic missense mutations in the TARDBP gene, which encodes the TDP-43 protein, have subsequently been identified as causative genetic mutations in both ALS and FTD. At the same time, the majority of patients with amyotrophic lateral sclerosis (ALS) and frontotemporal lobar disease (FTD) do not possess mutations in the TARDBP gene yet demonstrate widespread abnormalities involving TDP-43 (Gao et al., 2018). The stability, functionality, liquid-liquid phase separation (LLPS), and cellular localization of

TDP-43 are cooperatively regulated by self-oligomerization and RNA binding. However, how TDP-43 transitions from physiological to pathological states remains poorly understood (Pérez-Berlanga et al., 2022).

NPTX2

Neuronal pentraxins (NPs) were described as presynaptic receptors for taipoxin snake neurotoxins (Schlimgen et al., 1995). The NP family comprises several proteins, including NPTX2 (neuronal pentraxin 2), with an important role in activity dependent synaptic plasticity. NPTX2 is a secretory synaptic protein expressed presynaptically by pyramidal neurons and released at excitatory synapses (Chang et al., 2010). By forming a complex with NPTX1 and NPTXR, NPTX2 mediates AMPA receptor, clustering post-synaptically at GABAergic interneurons (O'Brien et al., 1999) Human NPTX protein is exclusively localized in the nervous system. Its central role is to regulate synaptogenesis, as well as to control glutamate signaling via the clustering of AMPA receptors. NPTX2 mediates synaptic maintenance, plasticity, and postsynaptic specialization in both inhibitory and excitatory synapses by binding to the neuronal pentraxin receptor (NPTXR) (Boiten et al., 2020). It is shown that the overall level of NPTX2 decreases with age and in dementia, however TDP-43 pathological neurons have increased levels of NPTX2 into the cytoplasm, possibly because of the loss of TDP-43 binding on NPTX2 mRNA (Hruska-Plochan et al., 2021).

Aim

Previous experiments in the research group of Prof. Polymenidou showed evidence for a positive correlation between NPTX2 and TDP-43 levels in TDP-43 overexpressing mature neurons and ALS and FTD patient brains (Hruska-Plochan et al., 2021). Since TDP-43 is shown to be essential for the development of mammalian organisms and play a key role in ALS and FTD, our aim is to investigate the effects of TDP-43 on NPTX2 levels during the differentiation of human neurons taking advantage of the neuronal model system established in Polymenidou lab (Wu et al., 2010; Geser et al., 2010). The qualitative results of this experiment will help us to further understand the link between TDP-43 and NPTX2 in healthy and pathological neural cells.

Materials & Methods

To achieve this aim, aging human neural networks established in Polymenidou lab (Dept. Of Quantitative biomedicine, UZH) were used to model TDP-43 proteinopathies in vitro. These neural networks are derived from iPSC-derived, colony morphology neural stem cells (iCoMoNSCs) established and well-characterized in Polimenidou Lab (Hruska-Plochan et al., 2021). This self-renewing human neural stem cell line was generated from induced pluripotent stem cells (iPSCs), originally derived from human skin fibroblast. Notably, the human neural model consists of self-organized and multi-layer glia and neural cultures with

synaptically connected and electrophysiologically active neurons, which then matures into a long-lived functional neural network over time. An important advantage of this system is its high reproducibility and significant longevity that makes it ideal to study neurodegenerative diseases such as ALS and FTD. Western Blotting and immunofluorescence were employed to quantify and visualize NPTX2 and TDP-43 levels in differentiating neural cell cultures under different transduction conditions (see *Fig. 3*).
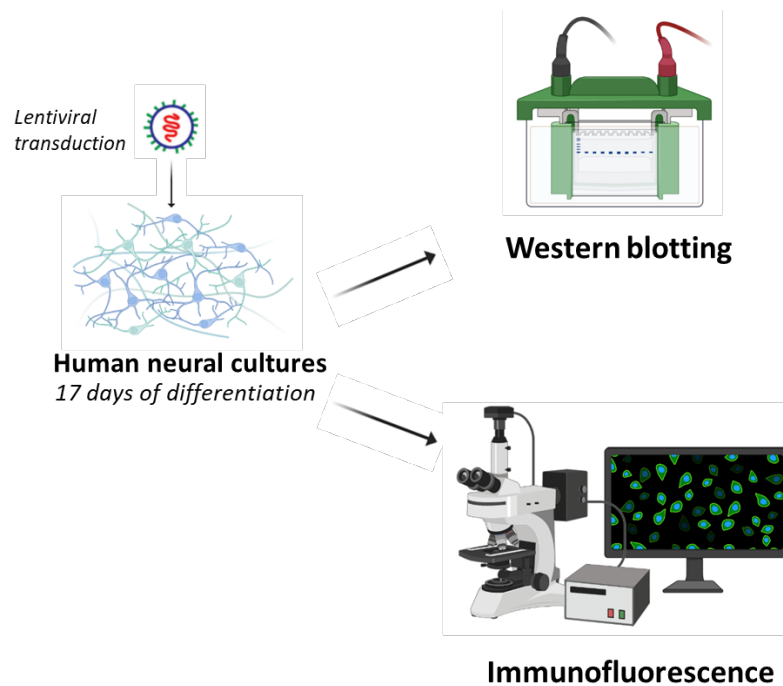

Fig 3: Experimental plan

Experimental Setup

Already grown and transduced human neural cultures were provided by the responsible Phd supervisor. In Polymenidou lab, in-house stock of iCoMoNSCs were plated on the first day in a 12-well plate for the Western Blot protocol and in a 96-well plate for the immunofluorescence protocol (see *Fig. 4*).
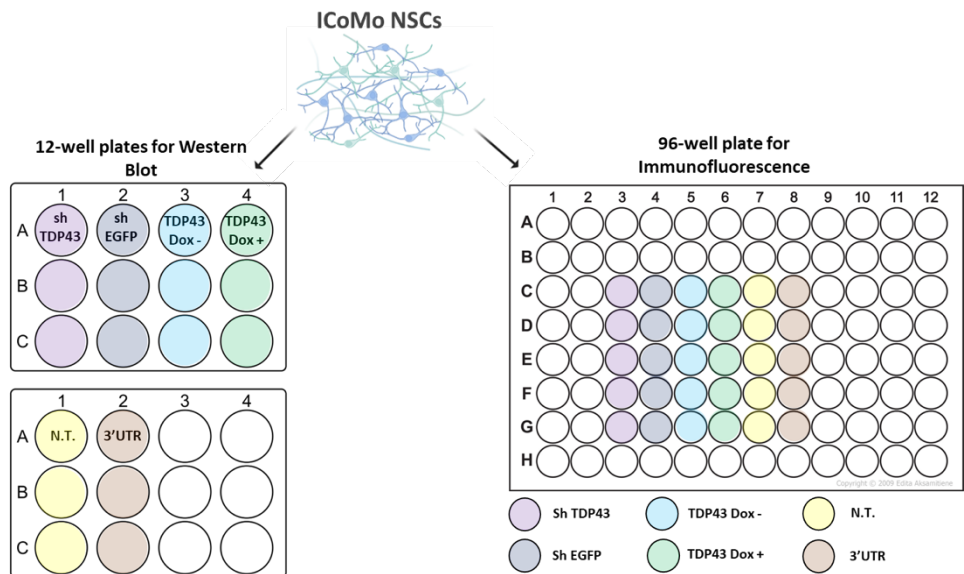
Fig 4: Experimental setup (cell culture plating)

On the 4th day, cell cultures were transduced with lentiviruses for 6 different conditions: *shTDP43*, *shEGFP*, *TDP43 dox-*, *TDP43 dox+*, WT and TDP-43 *3'UTR* (see *Fig. 4*). In the *shTDP43* condition the expression of TDP-43 was downregulated by transducing immature human neural cell culture with a short hairpin RNA (shRNA) targeting the mRNA of TDP-43. In the *shEGFP* condition, cells were transduced with an shRNA targeting the mRNA of the Enhanced Green Fluorescent Protein (EGFP) – this protein however is not normally present in the cells since they do not have the gene corresponding for EGFP translation; for this reason, this condition has been used as a control for the functioning of the shRNAs. In both *TDP43 dox+* and *TDP43 dox-* conditions, an additional gene sequence coding TDP-43 tagged with a small HA tag is transduced into the cells, however, only when Doxycycline is added the transgene can be expressed. Neurons were also transduced with TDP-43 in presence of its *3'UTR* that is responsible for TDP-43 autoregulation through a negative feedback loop, therefore in addition of Doxycycline TDP-43 is overexpressed but is also autoregulated. Lastly, as control neurons not transduced were also present. The *shEGFP*, the *TDP43 dox-* and the *NT* conditions serve as controls for the other three conditions. On the 5th day, the differentiation protocol was started and was interrupted at 17 days to generate immature differentiating human neural cultures (see *Fig. 5*).
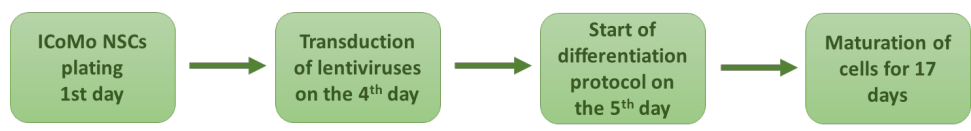

Fig 5: Cell culture preparation timeline representing stages of neuronal differentiation.

17 days after transduction, the culture contains differentiating neural cells, immature neurons and glial cells which are then used for the experiments. The full differentiation protocol would take 56 days during which the media composition is changed every day, adding growth

supplements in different concentrations to drive differentiation and growth of the culture. Before starting any of the following protocols mentioned below, each condition of the plates was visually checked under the EVOS M5000 Imaging System (Thermo Fisher Scientific) wide-field microscope to evaluate the presence of human neural networks in the wells (see *Fig. 6*).
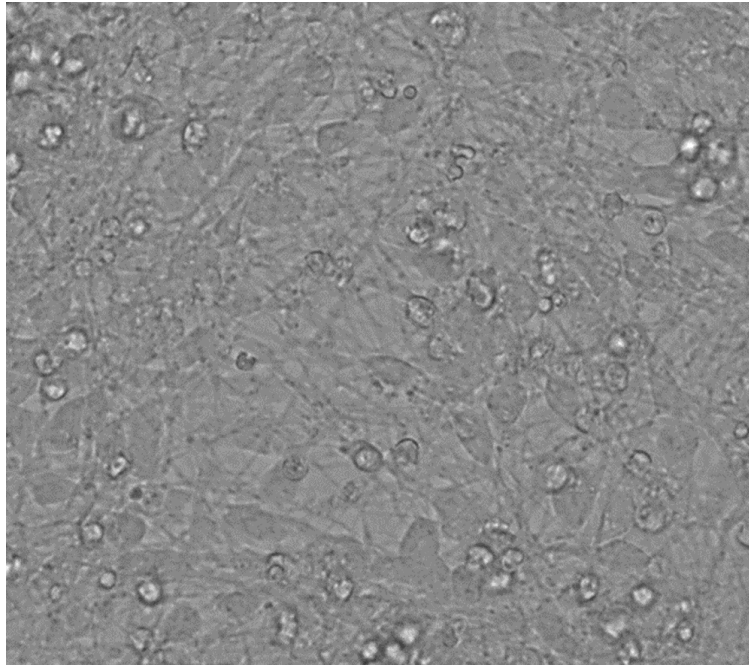

Fig 6: Bright field image displaying living differentiating neural stem cells a day prior to the execution of the experiment.

We began our protocols on the 17th day of the differentiation of the cultures before the cells became fully matured.

Immunofluorescence

For this experiment, the cell cultures were plated on a 96-well plate (Greiner). To fixate the culture on the 17th day of differentiation, PFA 16% was warmed up in a bead bath and added in a 1:4 dilution to each well, working under a chemical hood. After waiting 20 minutes, the PFA was discarded into a reservoir via a suction pump and the wells were washed with 250 μl of PBS for 10 minutes. Next, the wells were washed with 250 μl of 0.2% triton in PBS for another 10 minutes and then triton in PBS was discarded and 200 μl of blocking solution (5ml 10% donkey serum + 45ml 0.2% triton in PBS) was added per well for 1 hour. Two blocking solutions were prepared containing a different combination of opportune primary antibodies. The primary antibodies against MAP2 and NPTX2 were added in their respective amounts to both solutions to achieve their respective dilution (see *Tab. 1*). In one solution, the primary antibody against 3H8 was added (solution A) which targets the wild-type TDP-43 and in the other solution the antibody against HA was added (solution B) which specifically targets the transgenic TDP-43. Then, 100 ml of solution A was vortexed and added to each well of the

shTDP43, *TDP43 dox-* and the *NT* condition, whereas 100 ml of solution B was vortexed and added to each well of the *TDP43 dox+* and the *3'UTR* condition.

Table 1: Primary antibodies (I AB) for the immunofluorescence

Target	Antibody	Host	Ratio	Supplier, catalogue number
MAP2 (Neurons)	Anti-MAP2 antibody	Chicken (Ch)	1:1000	Lucerna Chem AG, ABC-ab5392-25 μL
NPTX2 polyclonal	Anti-NPTX2 polyclonal antibody	Rabbit (Rb)	1:200	Proteintech, 10889-1-AP-150 μL
HA Tag (transgenic TDP-43)	Anti-HA Tag monoclonal antibody	Mouse (Ms)	1:500	Thermo Fisher Scientific, 26183
3H8 C-Term TDP-43 (wild-type TDP-43)	Anti-TDP-43 (3H8) monoclonal antibody	Mouse (Ms)	1:200	Antibodies Online (Novus Biologicals), NBP1-92695

The plate was then incubated overnight in the cold room (4°C) on a shaker. On the following day, wells were washed three times with 250 μl PBS before it was removed, and 100 μl of vortexed secondary antibodies diluted in blocking solution was added per well (see *Tab. 2*). Afterwards, the plate was incubated for 1 hour at room temperature (~20°C) on a shaker, protected from light by wrapping it in aluminium foil. Four washes followed: (1) 200 μl 0.2% triton in PBS per well (2) 180 μl 0.2% triton in PBS + DAPI per well for 15-30 minutes (3) 200 ml 0.2% triton in PBS per well (4) 200 μl PBS per well. As a last step, 200 μl PBS was added before covering the plate with a plastic seal to protect it from contamination. The final cultures were stored in a cold room (4°C).

Table 2: Secondary antibodies (II AB) for the immunofluorescence

Antibody / Reagent	Host	Ratio	Supplier, catalogue number
Donkey anti-Chicken: Alexa Fluor® 647 AffiniPure F(ab')2 Fragment Donkey Anti-Chicken IgY (IgG) (H+L)	Chicken (Ch)	1:500	Jackson Immuno Research, AB_2340379
Donkey anti-Rabbit: Alexa Fluor® 568 Donkey Anti-Rabbit IgG (H+L) Antibody	Rabbit (Rb)	1:500	Thermo Fisher Scientific, A10042

Donkey anti-Mouse: Alexa Fluor® 488 Donkey Anti-Mouse IgG (H+L) Antibody	Mouse (Ms)	1:500	Thermo Fisher Scientific, A-21202
DAPI Solution (1 mg/mL)	-	1:500	Thermo Fisher Scientific, 62248

Immunofluorescence Imaging

The immunofluorescence images were taken with a CLSM-Leica SP8 inverse FALCON (Leica Microsystems) confocal microscope with a 63x magnification objective (Leica Microsystems) at a numerical aperture of 1.4na using oil as suspension media. Three channels were selected in the LEICA X software to minimize crosstalk (spectral overlap of the wavelength of different fluorophores) between the signal of different staining: (1st) DAPI at 405nm and HA/3H8 at 488nm (3rd) NPTX2 at 568nm MAP2 at 647nm (2nd). All the parameters were set optimally to achieve the ideal fluorescence intensity and optimal image quality: power of the laser beam for each channel, offset (to reduce background noise) and spectrum of wavelength emitted by the laser. The images were acquired in a 1848x1848 format, where the depth of the stacks was variable, but step size was 0.5μm for all stacks acquired. Images were edited in Fiji ImageJ for depiction purposes (Schindelin et al., 2012).

Western Blot

On the 17th day of differentiation, the neural cell culture was lysed in order to perform the Western Blot. The medium was removed from the cells and each well was washed with PBS. One tablet of Complete™ Mini EDTA-free Protease Inhibitor Cocktail and one tablet PhosSTOP™ were dissolved in 10ml RIPA buffer. Then the lysate solution for two 12-well plates (Greiner) was prepared by mixing 3.5μl RIPA lysis buffer, 14μl of Benzonase® Nuclease HC and 19.2 μl of $MgCl_2$. Subsequently, 200μl of that solution was added to each well. Then the cells were scraped from the wells and transferred into Eppendorf tubes. In order to completely lysate all the samples, the cells were mechanically disrupted in the Q500 Sonicator® (QSonica Sonicators) (elapsing time 3 min., amplitude 40%). Afterwards, protein concentration was quantified by using a BCA assay. The chemical mechanism behind it relies on two reactions. First, the peptide bonds in protein reduce Cu^{2+} ions from the Cu_2SO_4 to Cu^{1+}. The amount of reduced copper is proportional to the amount of protein in the sample. Second, the molecules of BCA (Bi-Cinchoninic Acid) form a purple-colored complex with the Cu^{1+} cations that strongly absorb light at a wavelength of 562 nm. The macromolecular structure of the proteins and the number of peptide bonds are reported to be responsible for color formation in the BCA. Accordingly, protein concentrations generally are determined and reported with reference to standards of a common protein such as bovine serum albumin (BSA). The progressive dilution in a linear manner of the BCA-Cu+ complex allows to create a standard curve in order to compare and determine unknown protein concentrations. To perform the BCA assay, the standard curve was made in a 96-well plate (Greiner) using BSA.

Row A of the plate was filled with BSA linearly diluted with water from 2000 µg/ml to 0 µg/ml. The wells in row B, C and D were then filled with 10µl of BSA solution taken from the corresponding well in row A in order to make three replicates and get the average concentration. The last well of row A was filled with 40 µl of RIPA lysis buffer. 40 µl of lysed cell solution was transferred to each well in row E in the 96-well plate. For every lysis sample three replicates were performed each 10 µl in order to get an average concentration. Concentrations obtained by a dilution series are depicted in *Fig. 7* below (concentrations in µg/ml).
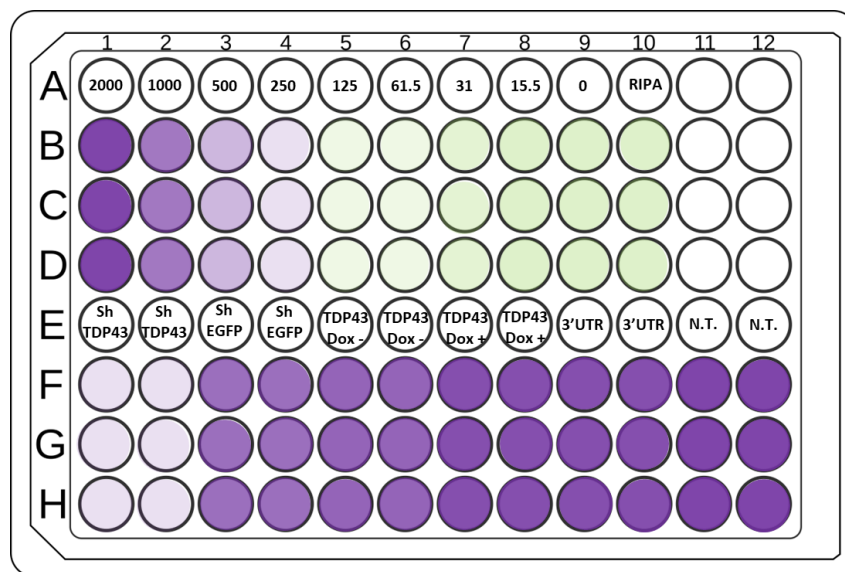

Fig 7: BCA assay scheme

After completion of the dilution series, 200µl of the mixture reagent given by the Pierce™ BCA Protein Assay Kit was added to each well. Incubation was done under light protection for 30 minutes at room temperature and subsequently, spectrophotometry was performed at 540-590nm using the Infinite 200 Pro® (Tecan) plate reader. The obtained calibration curve was used to equalize the amount of protein across the samples according to the following table (see *Tab. 3*):

Table 3: Protein sample preparation for Western Blot (amount per gel, final volume =30µl).

	Protein concentration 5 µg (µl)	Reducing agent (µl)	LSD sample buffer (µl)	RIPA (µl)
shTDP43 1	6.3	3	7.5	13.2
shTDP43 2	12.55	3	7.5	6.95
shEGFP 1	12.55	3	7.5	6.95
shEGFP 2	5.33	3	7.5	14.17
TDP43 dox- 1	4.54	3	7.5	14.96
TDP43 dox- 2	5.26	3	7.5	14.24
TDP43 dox+ 1	4.8	3	7.5	14.7

TDP43 dox+ 2	4.53	3	7.5	14.97
3'UTR 1	4.48	3	7.5	15
3'UTR 2	4.75	3	7.5	14.75
N.T. 1	3.95	3	7.5	15.55
N.T. 2	4.2	3	7.5	15.3

The Bolt™ Sample Reducing Agent (10X) and NuPAGE® LDS Sample Buffer (4X) was used for preparation of loading solutions. The equalized solutions were vortexed and spun, then incubated at 95°C for 10 minutes to let the proteins denature. The Sodium Dodecyl Sulphate - Polyacrylamide-Gel-Electrophoresis (SDS-PAGE) was performed on a 15-well NuPAGE™ 4-12% Bis-Tris Protein Gel using a 1X Bolt™ MES SDS Running Buffer. PageRuler™ Prestained Protein Ladder was used as a marker with known mass bands. By using a combination of sodium dodecyl sulfate (SDS) and polyacrylamide gel, it is possible to separate proteins solely based on their molecular weight, without the influence of structure and charge. SDS denatures proteins by disrupting non-covalent bonds and binding to amino acid side chains. Beta-mercaptoethanol is used to reduce disulphide bonds. The negative charge of the protein becomes proportional to its molecular weight. The solution is then loaded into the wells of a gel with a stacking and a separating component determined by Polyacrylamide concentration. In the stacking gel the proteins are collected so that they start running at the same time and in the separating gel they separate according to size. SDS masks intrinsic charge and confers similar charge-to-mass ratios to the proteins. Upon application of an electric field, the proteins migrate towards the anode, each with a different speed dependent on their mass. This straightforward technique allows for precise protein separation by mass. SDS-PAGE was run in a Mini Gel Tank (Thermo Fisher Scientific) for 10 minutes at 90V and then for around 30 minutes at 200V using the PowerPRO 300 Power Supply (Cleaver Scientific). After SDS-PAGE the gel was moved to the container with MilliQ water. Using the Regular nitrocellulose iBlot® 2 Transfer Stacks proteins were then transferred from the gel to a membrane by electrophoretic transfer in the iBlot™ 2 Gel Transfer Device for 7 minutes on 20V. The membranes were then cut and incubated for 1 hour at room temperature on a shaker completely submerged in the blocking buffer (5% milk in PBS-T). The blocking buffer allows to prevent all unspecific bounds during the following antibodies incubation. After blocking all the membranes, the samples were incubated over night with the respective primary antibodies which were diluted in 1% milk in PBS-T solution (see *Tab. 4*).

Table 4: Primary antibodies (I AB) for the Western Blot

Target	Antibody	Host	Ratio	Supplier, catalogue number
3H8 C-Term TDP-43	Anti-TDP-43 (3H8) monoclonal, mouse	Mouse	1:1000	Antibodies Online (Novus Biologicals), NBP1-92695
HA Tag	HA Tag Monoclonal Antibody	Rabbit	1:1000	Thermo Fisher Scientific, 26183
NPTX2 C-term	NPTX2 (NM_002523) (C-term)	Mouse	1:200	OriGene, SC122629
NPTX2 polyclonal	NPTX2 Polyclonal antibody	Rabbit	1:1000	Proteintech, 10889-1-AP-150UL
SOD	Rabbit anti Cu/Zn SOD polyclonal antibody	Rabbit	1:10'000	Enzo, Protein ID P00441
GAPDH	Anti-GAPDH antibody [6C5]	Mouse	1:2500	P4U-Lucerna Chem AG, ABC-ab8245-100uG

After incubation with primary antibodies, the membranes were washed 3 times for 15 minutes each with PBS-T. The secondary antibodies were diluted in 1% milk in PBS-T and subsequently added to each membrane for further incubation for 1 hour at room temperature (see *Tab. 5*). The secondary antibodies were conjugated with horseradish peroxidase (HRP) which converts luminol into 5-aminophthalic acid. Its electrons are in an excited state after conversion and subsequently transition to the ground state by releasing a detectable photon over time. After incubation with secondary antibodies, the membranes were washed 3 times for 15 minutes each with PBS-T. Then the development of the membranes was performed using Pico reagents, advancing to Femto reagents if necessary, and images were acquired in the Fusion FX (Vilber). The further processing of images was carried out using Fiji ImageJ (Schindelin et al., 2012).

Table 5: Secondary antibodies (II AB) for the Western Blot.

Antibody	Host	Ratio	Supplier, catalogue number
Goat anti-Mouse IgG (H+L) Secondary Antibody, HRP	Goat	1:5000	Thermo Fisher Scientific, 62-6520
Goat anti-Rabbit IgG (H+L) Cross-Adsorbed Secondary Antibody, HRP	Goat	1:10'000	Thermo Fisher Scientific, G-21234

Results

Western Blot

To present the quantitate analysis the Western Blot was performed. The images of obtained membranes have been processed in ImageJ. The measurements were normalized on GAPDH and SOD loading controls and subsequently averaged for their respective conditions. For each protein of interest (TDP-43 and NPTX2) we performed two Western Blots using antibodies targeting different regions of the proteins (see additional Western Blot results in the supplementary materials). The results of Western Blot clearly show that in the *shTDP43* condition the expression of TDP-43 is downregulated. On the contrary, the *TDP43 Dox On* condition shows the overexpression of TDP-43 and also the presence of tragments with smaller molecular weight (see *Fig. 8*).
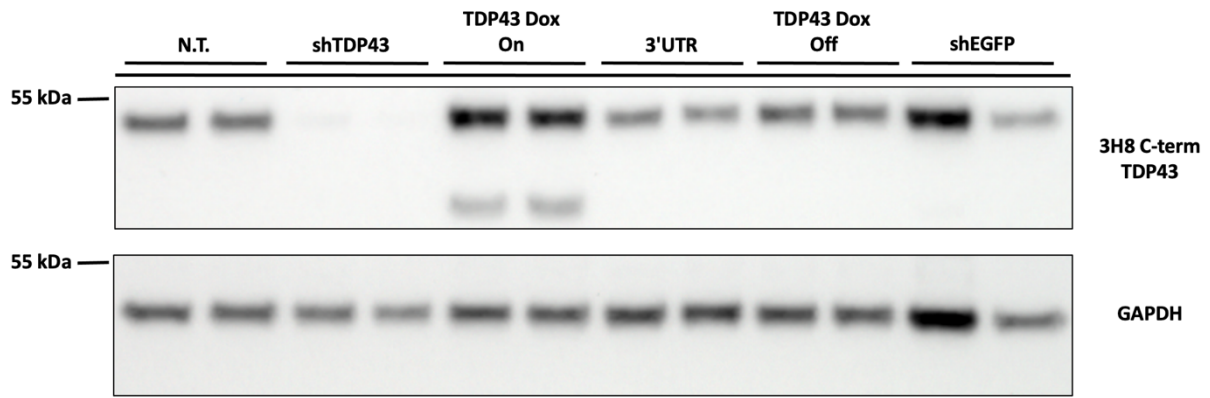
Figure 8: Western Blot performed using antibodies against 3H8 (marker for TDP-43). GAPDH was used as the loading control.

The following *Fig. 9* shows the overexpression of NPTX2 in only one condition (*TDP43 Dox On*) corresponding to overexpression of TDP-43.
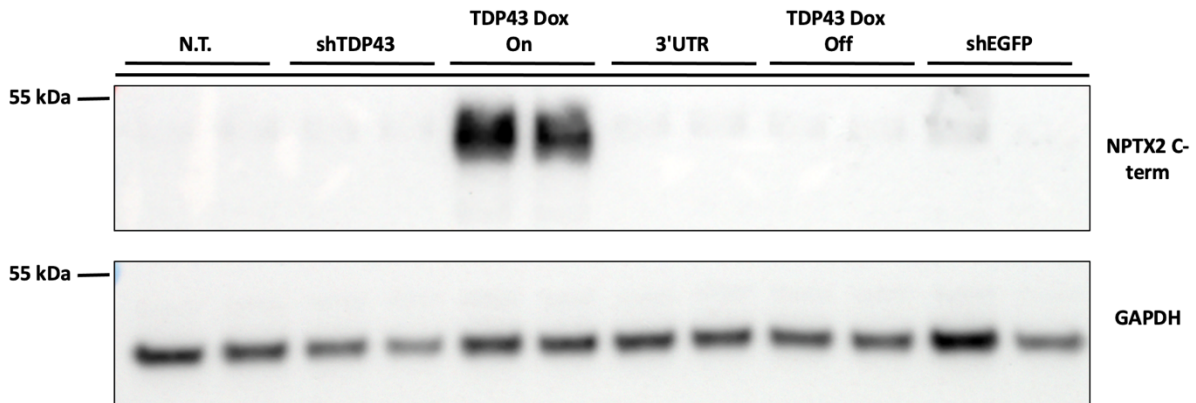

Figure 9: Western Blot performed using antibodies against NPTX2 (C-term). GAPDH was used as the loading control.

A quantification of the intensity of the bans normalized on GAPDH loading control was performed to fully evaluate TDP-43 and NPTX2 levels. The results show a significant increase in NPTX2 protein levels when TDP-43 is overexpressed (*TDP43 Dox On* condition) that shows increase of TDP-43 protein levels (see *Fig.10* and *Fig. 11*).
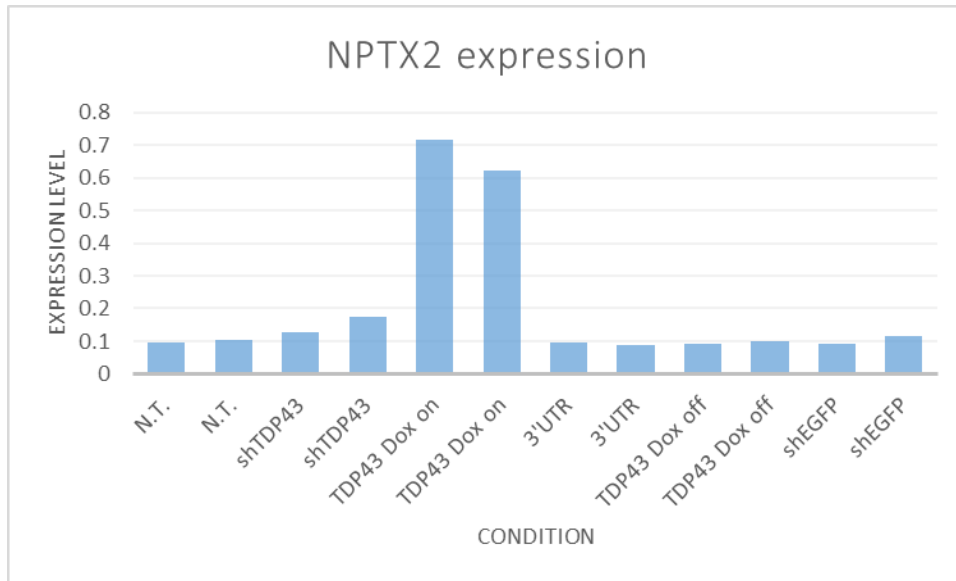
Figure 10: Quantification of the expression levels of NPTX2 in the NPTX2 Western Blot (*Fig. 9*).

Besides, the quantification of TDP-43 expression reveals again the decrease in the protein level in the downregulated cells corresponding to the *shTDP43* condition (see *Fig. 11*).

Figure 11: Quantification of the expression levels of TDP-43 in the TDP-43 Western Blot (*Fig. 8*).

Immunofluorescence

As soon as quantitative results were obtained with the Western Blots, we decided to perform a qualitative analysis with Immunofluorescence to visually investigate the results of our experiment. In the images from the human neural cell culture of the *TDP43 dox+* condition, we can clearly see in green several neurons which have been transduced and that are overexpressing TDP-43 mainly localized in the nucleus (see *Fig. 12B*). In some of those neurons positive for TDP-43 marked with white circles, we can observe an overlap with an

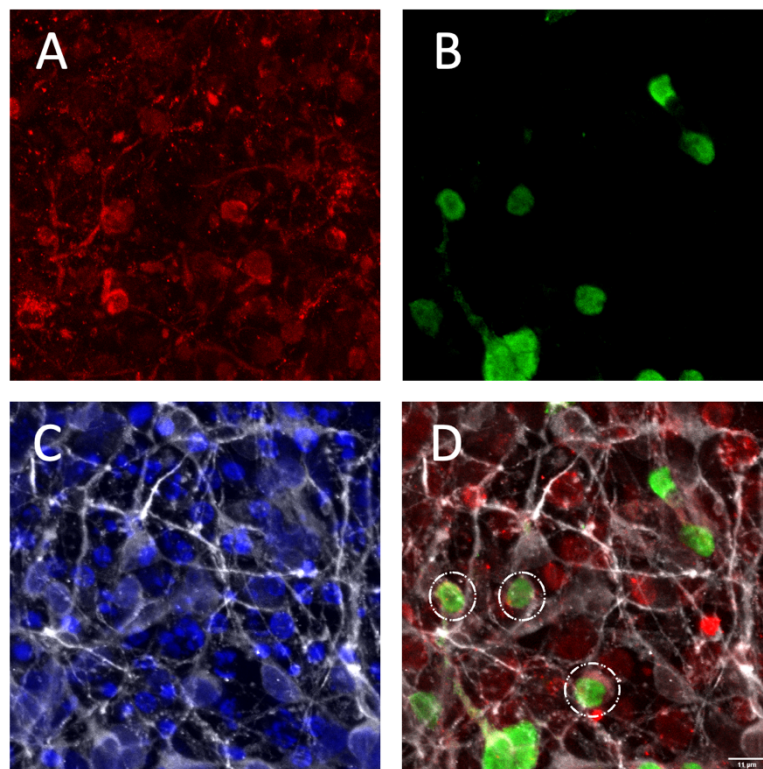increase in the presence of NPTX2 in the cytoplasm which we cannot observe in any other conditions (see *Fig. 12D*).

Figure 12: Four immunofluorescence images taken at 63x magnification of immature human neural cell culture overexpressing TDP-43 (*TDP43 dox+* condition) showing **(A)** NPTX2 (red), **(B)** TDP-43 HA (green), **(C)** DAPI (blue) + MAP2 (grey), **(D)** NPTX2 + TDP-43 HA + MAP2 (merge image). The four images show the exact same area, length reference in the lower right corner of **(D)**.

In the images of the control condition *TDP43 dox-* in which the cell culture is transduced with TDP-43 but is not induced with doxycycline, we can clearly see that the amount of the present TDP-43 is not as high as in the *TDP43 dox+* condition from before, displaying similar levels as for the TDP-43 present in WT condition (see *Fig. 13B and 14B*). Furthermore, we can observe a mostly unspecific signal for NPTX2 (see *Fig. 13A*).
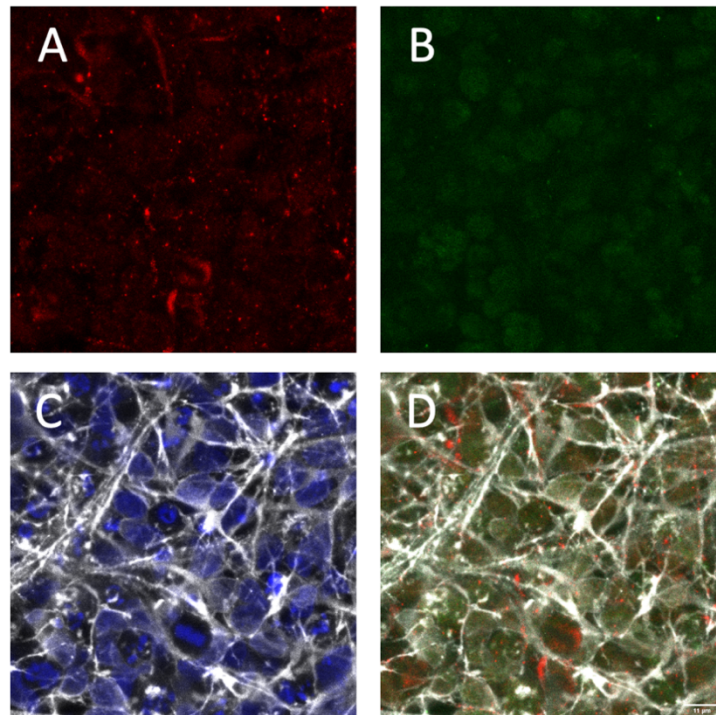
Figure 13: Four immunofluorescence images taken at 63x magnification of immature human neural cell culture transduced with TDP-43 but not induced (*TDP43 dox-* condition) showing **(A)** NPTX2 (red), **(B)** TDP-43 HA (green), **(C)** DAPI (blue) + MAP2 (grey,) **(D)** NPTX2 + TDP-43 HA + MAP2 (merge image). The four images show the exact same area, length reference in the lower right corner of **(D)**.

Regarding the *NT* condition (wild-type), another control condition, we can observe the presence of TDP-43 in all neurons on a normal level, mainly localized in the nucleus (see *Fig. 14B*). But here again, we can only observe a mostly unspecific signal of NPTX2 (see *Fig. 14A*). Also, in the *TDP43 3'UTR* condition with the human neural cell culture which overexpresses TDP-43 in the presence of its 3'UTR that allows for the autoregulation of TDP-43, we can appreciate the overexpression of TDP-43 in several neurons even though we cannot clearly appreciate the signal of NPTX2 (see *Fig. 15A and 15B*).
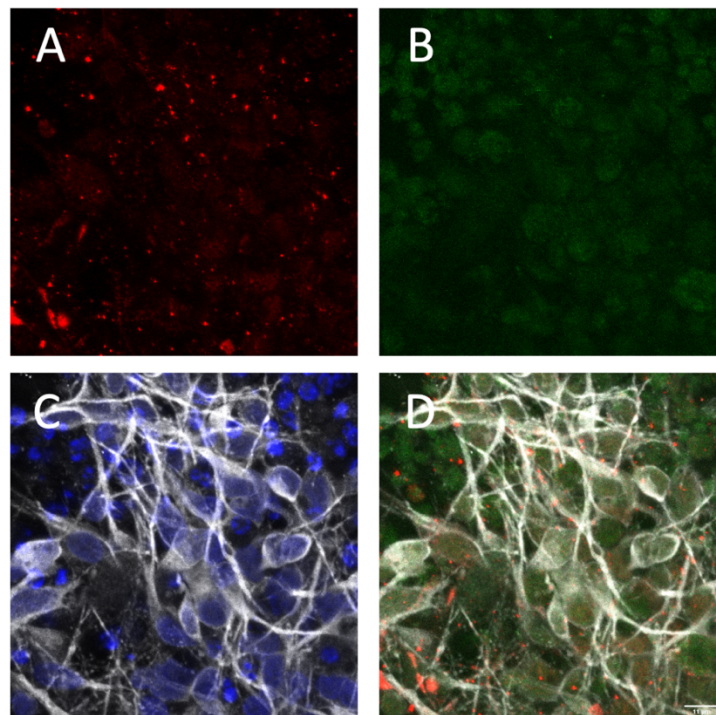
Figure 14: Four immunofluorescence images taken at 63x magnification of immature not transduced human neural cell culture *(wild type* condition) showing **(A)** NPTX2 (red), **(B)** TDP-43 HA (green), **(C)** DAPI (blue) + MAP2 (grey), **(D)** NPTX2 + TDP-43 HA + MAP2 (merge image). The four images show the exact same area, length reference in the lower right corner of **(D)**.
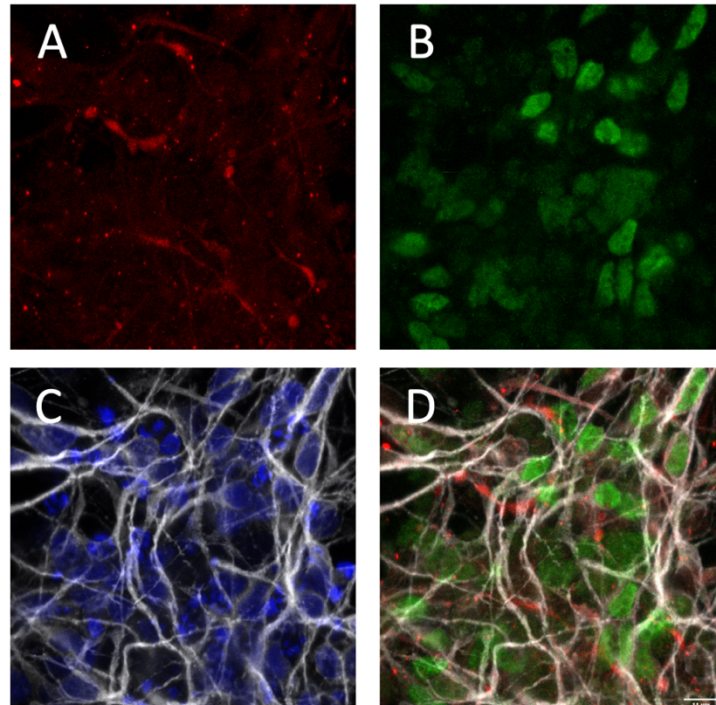

Figure 15: Four immunofluorescence images taken at 63x magnification of immature human neural cell culture overexpressing TDP-43 in presence of its 3'UTR (*TDP43 3'UTR* condition) showing **(A)** NPTX2 (red), **(B)** TDP-43 HA (green), **(C)** DAPI (blue) + MAP2 (grey), **(D)** NPTX2 + TDP-43 HA + MAP2 (merge image). The four images show the exact same area, length reference in the lower right corner of **(D)**.

When looking at the *shTDP43* condition where the shRNA targeting the mRNA of TDP-43, we can barely observe a clear signal of TDP-43 which seems to be less compared to the TDP-43 signal of the two control conditions before (see *Fig. 14B, 15B and 16B*). Additionally, the signal of NPTX2 also is barely noticeable compared to the unspecific signal of NPTX2 in the control conditions (see *Fig. 14A, 15A and 16A*).
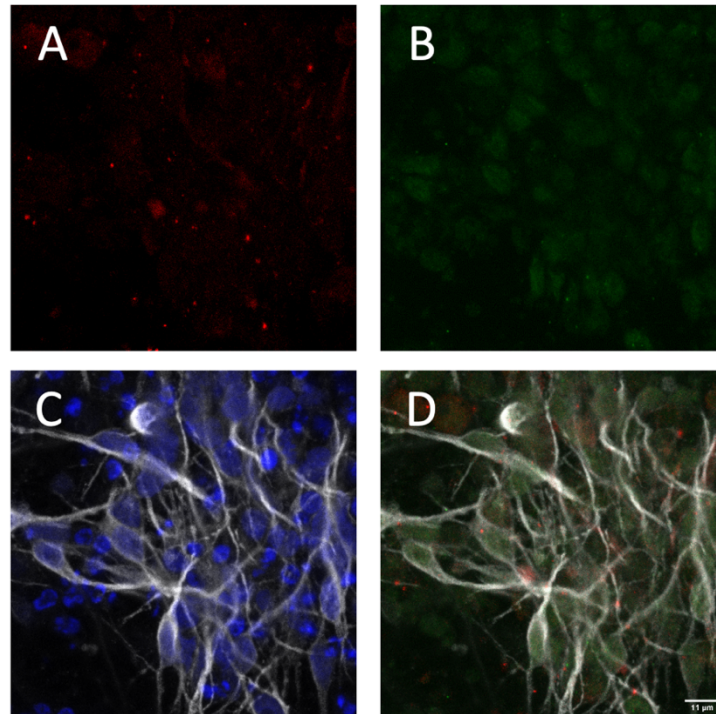

Figure 16: Four immunofluorescence images taken at 63x magnification of immature human neural cell culture transduced with shRNA targeting TDP-43 (*shTDP43* condition) showing **(A)** NPTX2 (red), **(B)** TDP-43 HA (green), **(C)** DAPI (blue) + MAP2 (grey), **(D)** NPTX2 + TDP-43 HA + MAP2 (merge image). The four images show the exact same area, length reference in the lower right corner of **(D)**.

In the last control condition, the *shEGFP* condition, we can again observe a TDP-43 signal which is comparable to the TDP-43 signal of the other two control conditions, *TDP43 dox-* and *NT* mainly localized in the nucleus (see *Fig. 13B, 14B* and *17B*). Here again, we can only observe a mostly unspecific signal for NPTX2 (see *Fig. 17A*).
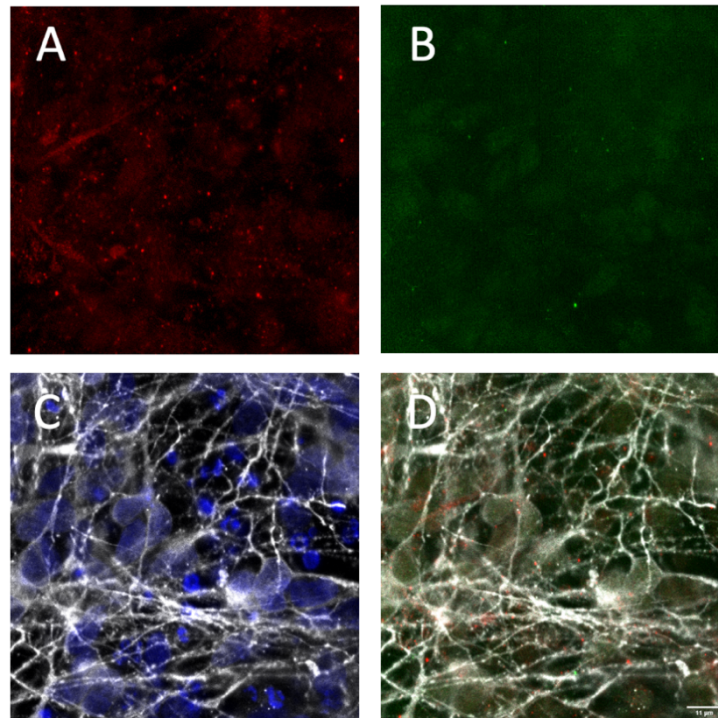
Figure 17: Four immunofluorescence images taken at 63x magnification of immature human neural cell culture transduced with shRNA targeting EGFP (*shEGFP* condition) showing **(A)** NPTX2 (red), **(B)** TDP-43 HA (green), **(C)** DAPI (blue) + MAP2 (grey), **(D)** NPTX2 + TDP-43 HA + MAP2 (merge image). The four images show the exact same area, length reference in the lower right corner of **(D)**.

Discussion

The results we obtained from the immunofluorescence and the Western Blot support each other and together prove that it is possible to perform both protocols on differentiating neurons at day 17, a stage that has been for the first time investigated in Polymenidou lab with this project. The western blot quantitative analysis, along with the immunofluorescence images are in line with previous studies performed in mature human neurons in Polymenidou Lab (Hruska-Plochan et al., 2021), proving the correlation between TDP-43 overexpression and increasing accumulation of NPTX2 into the cytoplasm not only of mature neurons but also while neural cultures are still differentiating (Fig 12D). From these results, we can infer that lentiviruses can still be used to transduce immature neurons in the model system and that it can further be taken advantage of and built upon for further investigations. We could further observe that not all neurons that were overexpressing TDP-43 showed an overlap with increased levels of NPTX2. This is most likely due to multiple reasons, one of them being the differentiation stage of the model system used, since only cells that are almost in a neuronal stage can overexpress NPTX2. This however needs further investigation in order to validate this assumption. For this reason a future experiment needs to be performed in which different timepoint are taken into consideration for the analysis. Another possible reason is related to the specificity and correct functioning of the NPTX2 antibody. We evaluated that the NPTX2 antibody used for the staining in the cell cultures for the immunofluorescence did not produce a reliable strong and continuous signal. For most conditions, we could only observe a mostly

unspecific signal of NPTX2 (see *Fig. 13-17A*). We therefore propose to improve the detection of NPTX2 by either trying multiple different antibodies targeting NPTX2 and validating the quality of the signal pre-emptively. Possible future experiments are needed which repeat the protocols we performed while looking at multiple different timepoints throughout the differentiation process of the model system. This way not only could the total count of surviving cells and the cell population dynamics be observed, but the temporal component and dynamics of TDP-43 and NPTX2 levels could be investigated too. By evaluating the behavior of the differentiating cells over time while quantifying expression levels, further insight into mechanisms of action, correlations, and importance of TDP-43 and NPTX2 can be achieved.

References

Afroz T, Pérez-Berlanga M, Polymenidou M. Structural Transition, Function and Dysfunction of TDP-43 in Neurodegenerative Diseases. Chimia (Aarau). 2019 May 29;73(6):380-390. doi: 10.2533/chimia.2019.380. PMID: 31118120.

Boiten WA, van Steenoven I, Xiao MF, Worley PF, Noli B, Cocco C, Ferri GL, Lemstra AW, Teunissen CE. Pathologically Decreased CSF Levels of Synaptic Marker NPTX2 in DLB Are Correlated with Levels of Alpha-Synuclein and VGF. Cells. 2020 Dec 29;10(1):38. doi: 10.3390/cells10010038. Erratum in: Cells. 2022 Feb 14;11(4): PMID: 33383752; PMCID: PMC7824459.

Chang MC, Park JM, Pelkey KA, Grabenstatter HL, Xu D, Linden DJ, Sutula TP, McBain CJ, Worley PF. Narp regulates homeostatic scaling of excitatory synapses on parvalbumin-expressing interneurons. Nat Neurosci. 2010 Sep;13(9):1090-7. doi: 10.1038/nn.2621. Epub 2010 Aug 22. PMID: 20729843; PMCID: PMC2949072.

De Boer EMJ, Orie VK, Williams T, Baker MR, De Oliveira HM, Polvikoski T, Silsby M, Menon P, van den Bos M, Halliday GM, van den Berg LH, Van Den Bosch L, van Damme P, Kiernan MC, van Es MA, Vucic S. TDP-43 proteinopathies: a new wave of neurodegenerative diseases. J Neurol Neurosurg Psychiatry. 2020 Nov 11;92(1):86–95. doi: 10.1136/jnnp-2020-322983. Epub ahead of print. PMID: 33177049; PMCID: PMC7803890.

Gao J, Wang L, Huntley ML, Perry G, Wang X. Pathomechanisms of TDP-43 in neurodegeneration. J Neurochem. 2018 Feb 27:10.1111/jnc.14327. doi: 10.1111/jnc.14327. Epub ahead of print. PMID: 29486049; PMCID: PMC6110993.

Geser F, Lee VM, Trojanowski JQ. Amyotrophic lateral sclerosis and frontotemporal lobar degeneration: a spectrum of TDP-43 proteinopathies. Neuropathology. 2010 Apr;30(2):103-12. doi: 10.1111/j.1440-1789.2009.01091.x. Epub 2010 Jan 25. PMID: 20102519; PMCID: PMC3131978.

Hruska-Plochan M, Betz K., Ronchi K., Wiersma V., Maniecka Z., Hock E., Laferriere F., Sahadevan S., Hoop V., Delvendahl I., Panatta M., Bourg A., Bohaciakova D., Frontzek K., Aguzzi A., Lashley T., Robinson M., Karayannis T., Mueller M., Hierlemann A, Polymenidou M. bioRxiv 2021.12.08.471089; doi: 10.1101/2021.12.08.471089

Laferrière, F., Maniecka, Z., Pérez-Berlanga, M. *et al.* TDP-43 extracted from frontotemporal lobar degeneration subject brains displays distinct aggregate assemblies and neurotoxic effects reflecting disease progression rates. *Nat Neurosci* 22, 65–77 (2019). https://doi.org/10.1038/s41593-018-0294-y

Ling SC, Polymenidou M, Cleveland DW. Converging mechanisms in ALS and FTD: disrupted RNA and protein homeostasis. Neuron. 2013 Aug 7;79(3):416-38. doi: 10.1016/j.neuron.2013.07.033. PMID: 23931993; PMCID: PMC4411085.

Mejzini R, Flynn LL, Pitout IL, Fletcher S, Wilton SD, Akkari PA. ALS Genetics, Mechanisms, and Therapeutics: Where Are We Now? Front Neurosci. 2019 Dec 6;13:1310. doi: 10.3389/fnins.2019.01310. PMID: 31866818; PMCID: PMC6909825.

Mitchell JD, Borasio GD. Amyotrophic lateral sclerosis. Lancet. 2007 Jun 16;369(9578):2031-2041. doi: 10.1016/S0140-6736(07)60944-1. PMID: 17574095.

O'Brien RJ, Xu D, Petralia RS, Steward O, Huganir RL, Worley P. Synaptic clustering of AMPA receptors by the extracellular immediate-early gene product Narp. Neuron. 1999 Jun;23(2):309-23. doi: 10.1016/s0896-6273(00)80782-5. PMID: 10399937.

Olney NT, Spina S, Miller BL. Frontotemporal Dementia. Neurol Clin. 2017 May;35(2):339-374. doi: 10.1016/j.ncl.2017.01.008. PMID: 28410663; PMCID: PMC5472209.

Prasad A, Bharathi V, Sivalingam V, Girdhar A, Patel BK. Molecular Mechanisms of TDP-43 Misfolding and Pathology in Amyotrophic Lateral Sclerosis. Front Mol Neurosci. 2019 Feb 14;12:25. doi: 10.3389/fnmol.2019.00025. PMID: 30837838; PMCID: PMC6382748.

Pérez-Berlanga M, Laferrière F, Polymenidou M. SarkoSpin: A Technique for Biochemical Isolation and Characterization of Pathological TDP-43 Aggregates. Bio Protoc. 2019 Nov 20;9(22):e3424. doi: 10.21769/BioProtoc.3424. PMID: 33654921; PMCID: PMC7853943.

Pérez-Berlanga M, Wiersma V I, Zbinden A, Vos L, Wagner U, Foglieni C, Mallona I, Betz K, Cléry A, Weber J, Guo Z, Rigort R, Rossi P, Tantardini E, Sahadevan S, Stach O, Hruska-Plochan M, Allain, Polymenidou M. TDP-43 oligomerization and RNA binding are codependent but their loss elicits distinct pathologies. BioRxiv 2022) May 493029. doi.org/10.1101/2022.05.23.493029

Schindelin, J., Arganda-Carreras, I., Frise, E., Kaynig, V., Longair, M., Pietzsch, T., … Cardona, A. (2012). Fiji: an open-source platform for biological-image analysis. *Nature Methods*, *9*(7), 676–682. doi:10.1038/nmeth.2019

Schlimgen AK, Helms JA, Vogel H, Perin MS. Neuronal pentraxin, a secreted protein with homology to acute phase proteins of the immune system. Neuron. 1995 Mar;14(3):519-26. doi: 10.1016/0896-6273(95)90308-9. PMID: 7695898.

Sephton CF, Good SK, Atkin S, Dewey CM, Mayer P 3rd, Herz J, Yu G. TDP-43 is a developmentally regulated protein essential for early embryonic development. J Biol Chem. 2010 Feb 26;285(9):6826-34. doi: 10.1074/jbc.M109.061846. Epub 2009 Dec 29. Erratum in: J Biol Chem. 2010 Dec 3;285(49):38740. PMID: 20040602; PMCID: PMC2825476.
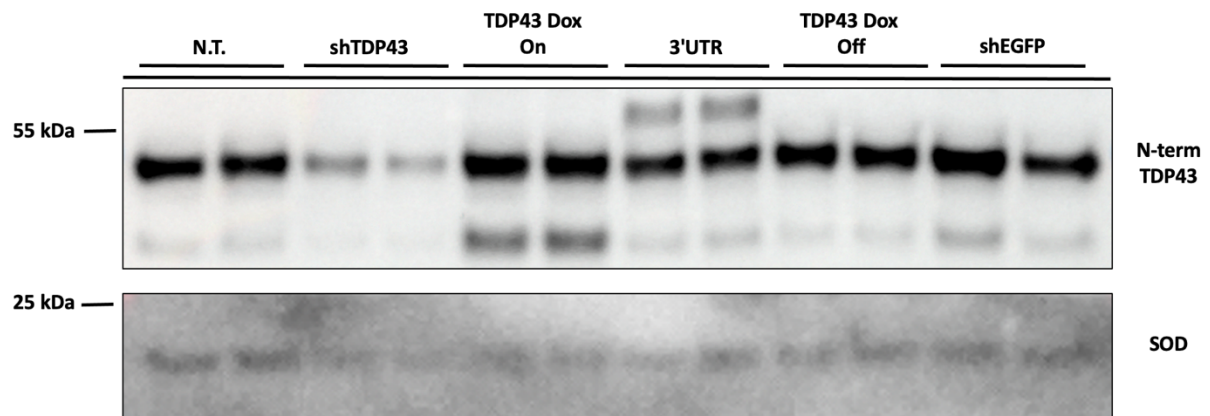
Van Damme P, Robberecht W. Recent advances in motor neuron disease. Curr Opin Neurol. 2009 Oct;22(5):486-92. doi: 10.1097/WCO.0b013e32832ffbe3. PMID: 19593125.

Wu LS, Cheng WC, Hou SC, Yan YT, Jiang ST, Shen CK. TDP-43, a neuro-pathosignature factor, is essential for early mouse embryogenesis. Genesis. 2010 Jan;48(1):56-62. doi: 10.1002/dvg.20584. PMID: 20014337.
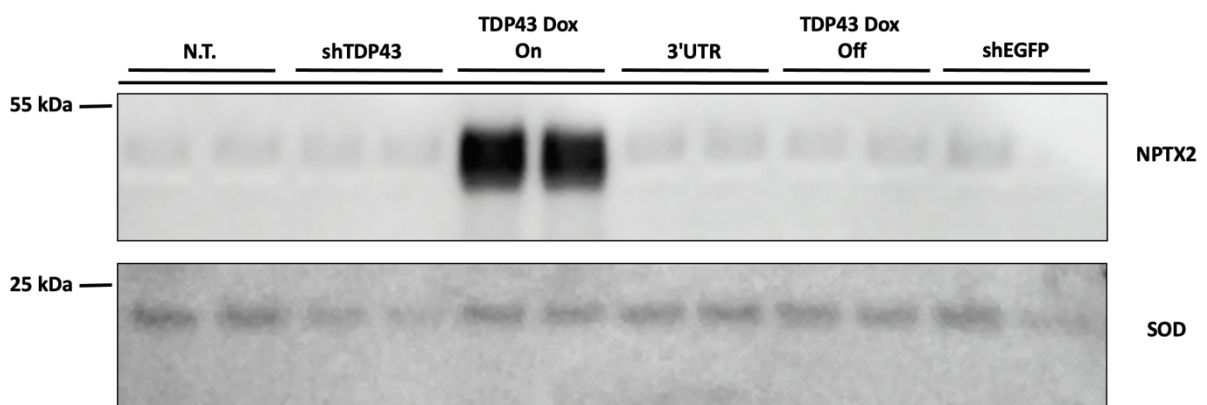
Younes K, Miller BL. Frontotemporal Dementia: Neuropathology, Genetics, Neuroimaging, and Treatments. Psychiatr Clin North Am. 2020 Jun;43(2):331-344. doi: 10.1016/j.psc.2020.02.006. Epub 2020 Apr 8. PMID: 32439025.

Appendix

Supplementary Figures

Supplementary Figure 1: Western Blot performed using antibodies against HA (marker for TDP-43 N-term). SOD was used as the loading control.

Supplementary Figure 2: Western Blot performed using antibodies against NPTX2. SOD was used as the loading control.

Supplementary Material

Supplementary Table 1: Reagents

Reagent	Supplier, catalogue number
PFA 16%	Thermofischer Scientific, 28908
PBS (10X), pH 7.4	Thermo Fisher Scientific, 70011044
PBS-T	PBS with 0,02 Tween-20
Triton X100	Sigma Aldrich, T9284
Donkey serum	Merck, S30
RIPA Buffer	10 mM Tris, pH 7.4 100 mM NaCl 1 mM EDTA 1 mM EGTA 1% Triton X-100 10% glycerol 0.1% SDS 0.5% deoxycholate
Benzonase® Nuclease HC, Purity ¿ 90%	Merck, 71205-3, 25 KU
Complete™, Mini, EDTA-free Protease, Inhibitor Cocktail	Roche, 11836170001
PhosSTOP™	Merck (Roche), 4906845001
Pierce™ BCA Protein Assay Kit	Thermo Fisher Scientific, 23227
Bolt™ Sample Reducing Agent (10X)	Thermo Fisher Scientific, B0009
NuPAGE® LDS Sample Buffer (4X)	Thermo Fisher Scientific, NP0007
NuPAGE™ 4-12% Bis-Tris Protein Gels 1.0 mm, 15-well	Thermo Fisher Scientific, NP0323PK2

iBlot® 2 Transfer Stacks, nitrocellulose, regular size	Thermo Fisher Scientific, IB23001
Thermo Scientific™ PageRuler™ Plus Prestained Protein Ladder, 10 to 250 kDa	Thermo Fisher Scientific, 26619
SuperSignal™ West Pico PLUS Chemiluminescent Substrate	Thermo Fisher Scientific, 34579
SuperSignal™ West Femto Maximum Sensitivity Substrate	Thermo Fisher Scientific, 34094

Supplementary Table 2: Machines & Instruments

Name	Manufacturer
EVOS M5000 Imaging System (Widefield microscope)	Thermo Fisher Scientific
CLSM-Leica SP8 inverse FALCON	Leica Microsystems
Eppendorf ThermoMixer® C	Eppendorf
Q500 Sonicator®	QSonica Sonicators
Infinite 200 Pro®	Tecan
Mini Gel Tank	Thermo Fisher Scientific
PowerPRO 300 Power Supply, 300V, 700mA, 150W	Cleaver Scientific
iBlot™ 2 Gel Transfer Device	Thermo Fisher Scientific
Fusion FX	Vilber